The Knee 26 (2019) 969–977

Contents lists available at ScienceDirect

The Knee

The interrelationship between anterior cruciate ligament tibial footprint and anterolateral meniscal root insertions: Quantitative, morphological and positional analyses using three-dimensional computed tomography images

Keiji Tensho *, Tomoya Iwaasa, Suguru Koyama, Kazushige Yoshida, Hiroki Shimodaira, Hiroshi Horiuchi, Hiroyuki Kato, Naoto Saito, Nanae Fukushima

Department of Orthopedic Surgery, Shinshu University School of Medicine, Nagano, Japan

ARTICLE INFO

Article history:
Received 23 March 2019
Received in revised form 18 June 2019
Accepted 3 July 2019

Keywords:
Anterior cruciate ligament
Tibial footprint
Anterolateral meniscal root
Three-dimensional computed tomography

ABSTRACT

Background: The purpose of this study was to evaluate quantitative, morphological and positional differences between the anterior cruciate ligament (ACL) tibial footprint and anterolateral meniscal root (ALMR) insertion and investigate an intraoperative landmark to estimate their boundaries.

Methods: Thirty-three fixed human cadaveric knees were evaluated. After resecting the components, the anterior fiber (AF) and posterior fiber (PF) of ALMR, the tibial center of ACL bundles (anteromedial (AM) and posterolateral (PL) bundles) and ACL were marked. Insertion morphology was classified into three categories, and the distance and relative positional relationship between AF/PF insertions and the center of each attachment were measured on three-dimensional computed tomography images.

Results: There was no significant difference between the AF of AM and ACL ($P = 0.16$), but both were significantly shorter than the AF of PL (both $P < 0.001$). There was no significant difference between the PF of ACL and PL ($P = 0.99$), which were significantly shorter than PF of AM (both $P < 0.001$). Morphology of the ACL tibial insertion was classified as follows: triangular, 15 knees (45.5%); oval, 18 knees (54.5%); none, C-shape. Quantitative and positional analyses showed that the AF insertion was significantly closer to AM and ACL centers in the oval type than in the triangular type. Excluding two cases, the AF/PF insertion was located laterally to the ML center of the medial and lateral intercondylar tubercles.

Conclusion: Proximity of ACL tibial footprint and ALMR varies by their footprint morphology. The medial and lateral intercondylar tubercles were useful landmarks for ALMR injury prevention.

* Corresponding author at: Department of Orthopedic Surgery, Shinshu University School of Medicine, 3-1-1 Asahi Matsumoto-shi, Nagano 390-8621, Japan.
E-mail address: kten@shinshu-u.ac.jp. (K. Tensho).

https://doi.org/10.1016/j.knee.2019.07.004
0968-0160/

1. Introduction

Many studies have been conducted on the detailed anatomy of anterior cruciate ligament (ACL) footprint and the surrounding structures [1–4], and practicing surgeons should have a thorough knowledge of such anatomy. On the tibial side, the footprint morphology, size, and fiber arrangement vary widely among patients, further complicated by their various surrounding tissues compared to the femoral side [5–7].

Several authors have reported on the detailed anatomy of bony/anatomical structures around the ACL tibial footprint and found that this footprint is adjacent to the anterolateral meniscal root (ALMR) insertion [8–14]. Among these reports, the

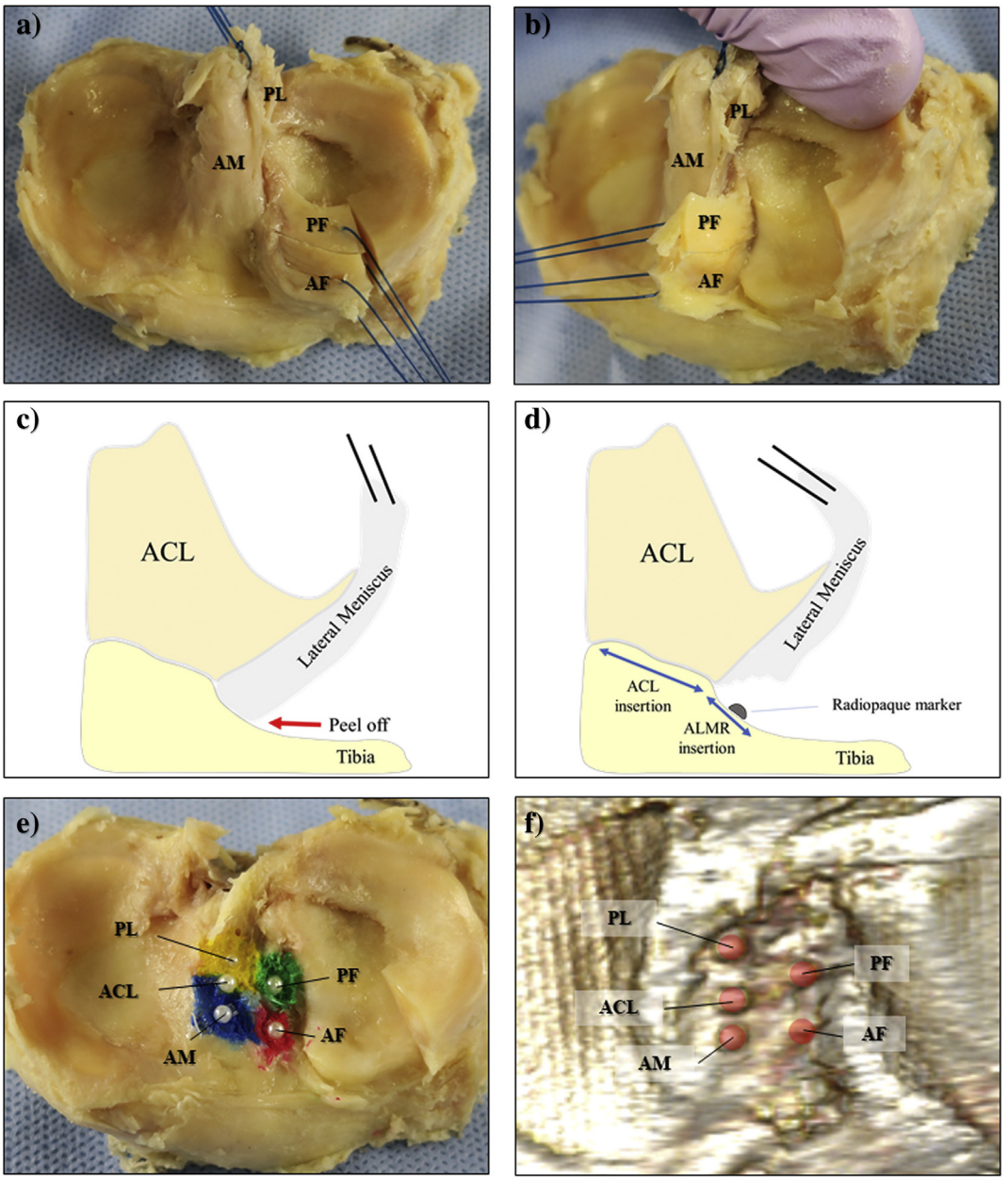

Figure 1. Macroscopic gross appearance and three-dimensional computed tomography images of the left knee's tibial plateau. (a) The anterior horn of the lateral meniscus was transected three centimeters from the insertion at half-width and divided into the anterior fiber (AF) and posterior fiber (PF) of the anterolateral meniscal root (ALMR). (b) AF and PF were turned over to expose the bony insertion. (c) Diagram of the boundary between ALMR insertion and anterior cruciate ligament (ACL) as seen from the anterior; ALMR is flipped over and separated from the bony surface. (d) A radiopaque marker is applied to the insertion where the continuity between the meniscus and the bone is lost. (e) Each attachment of fiber bundle marked with radiopaque marker. (f) Three-dimensional imaging of same sites.

proximity, overlap, and complex interrelationship between the ACL tibial footprint and ALMR have been reported, in addition to the risk of damage during bone tunnel drilling [15–17]. In a study using cadaveric knees, LaPrade et al. suggested the risk of damage to the lateral meniscus when creating a bone tunnel at the center of the tibial footprint [16], and there have been several similar reports of damage to the lateral meniscus in a clinical context [18,19].

However, because the anterior horn of the lateral meniscus is broadly attached to the lateral side of the ACL tibial footprint, its detailed and quantitative positional relationships with the center of each ACL fiber bundle are unknown. In addition, this relationship can also change due to the diverse morphology of the ACL tibial footprint. In terms of arthroscopic surgery, boundaries between these structures are unclear, and intraoperative landmarks for estimating the boundary between them have not been investigated. The present study was performed to evaluate quantitative, morphological and positional differences between the ACL tibial footprint and ALMR insertion, and investigate an intraoperative landmark to estimate their boundaries. We hypothesized that the proximity between the ACL tibial footprint and ALMR may vary according to the footprint morphology.

2. Materials and methods

2.1. Specimen collection and preparation

To investigate the correlation between ACL tibial footprint and anterior horn of lateral meniscus, an anatomic study using embalmed cadaveric knees was performed. Knees that displayed macroscopic degenerative changes or evidence of trauma, such as osteoarthritis, meniscal tears, and discoid lateral meniscus or ligament injury were excluded from this study. Thirty-

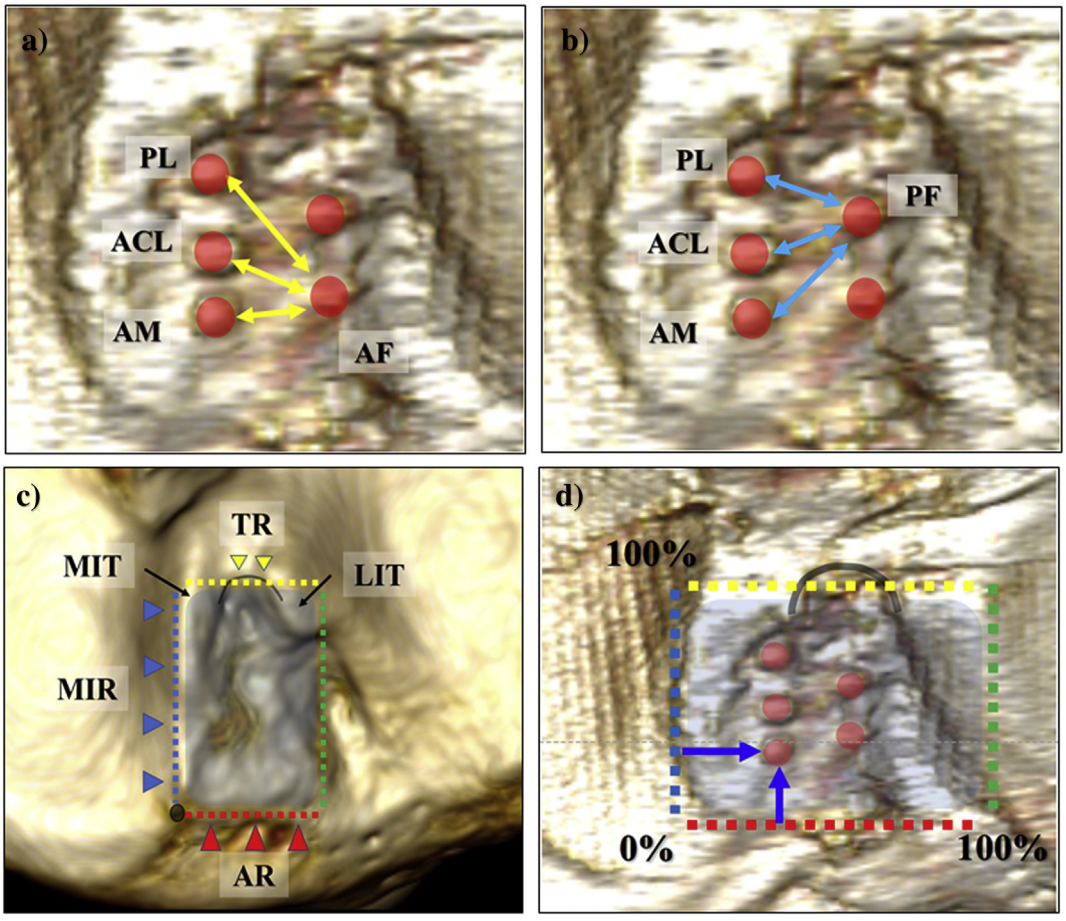

Figure 2. Axial view and expansion of the intercondylar area in three-dimensional computed tomography images of the left knee's tibial plateau. (a, b) Distance from each center of anterior cruciate ligament (ACL) fiber to the center of the anterior fiber (AF) and posterior fiber (PF) insertions. (c) Configuration of grid in the intercondylar area. (d) Positions were each determined by the relative distances from the medial and anterior reference lines. Blue arrow, medial intercondylar ridge (MIR); blue dotted line, line aligned to MIR; red arrow, anterior ridge (AR); red dotted line, line aligned to AR and intersecting perpendicularly to blue dot line; yellow arrow, ACL tibial ridge (TR); yellow dotted line, line in contact with anterior margin of the TR and intersecting perpendicularly to the blue dotted line; green dotted line, line in contact with the lateral margin of the lateral intercondylar tubercle (LIT) and intersecting perpendicularly to the red and yellow dotted lines; black dot, intersection point between MIR and AR. (For interpretation of the references to color in this figure legend, the reader is referred to the web version of this article.)

three non-paired knees with intact ACL from 33 adult cadaveric specimens (20 males, 13 females) were used. The average age was 85.7 years (range, 60–97). Of these cadaveric specimens, there were 18 right knees and 15 left knees. The muscle and capsule around the knee and posterior cruciate ligament were removed. After the ACL was divided into the anteromedial bundle (AMB) and posterolateral bundle (PLB), the ligament was cut at the femoral attachment from the roof of the intercondylar notch. The proximal tibia was cut 30 mm from the articular surface with a bone saw in the axial plane. The anterior horn of the lateral meniscus was cut at 30 mm from the root in the transverse direction. Additionally, in order to evaluate the interrelationship of the ACL tibial footprint and ALMR insertion in detail, the meniscus was cut at half-width in the longitudinal direction to the root attachment and divided into the following two parts: anterior fiber (AF) and posterior fiber (PF) which were renamed for clarity from 'inner and outer fibers' as originally described by Fujishiro et al. (Figure 1(a)). Each of the two parts was sutured with 1-0 nylon thread, turned over, and the AF was carefully peeled from the bony insertion of the bony side using a scalpel [8] (Figure 1(b), (c)). When the continuity of the meniscus/bone was interrupted and only the ACL from the articular side was connected, the area of the footprint for each peeled insertion was marked with surgical ink (Figure 1(d)). Subsequently, the PF and the AMB and PLB of ACL were peeled from the tibial attachment and likewise marked with surgical ink. Marking was carried out with a radiopaque marker in the central section within the marked area (Figure 2(a)). The midpoint between the center of the AMB and PLB was defined and marked as the center of the ACL. Macroscopic images were obtained, and the morphology of the ACL footprint was classified as either oval, triangular, or C-shaped, as previously described [7]. Three experienced orthopedic surgeons (TI, SK, and HS) performed morphological evaluations, and the morphological type was determined by two of three observers.

2.2. Micro-computed tomography analyses and evaluation

All specimens were scanned at a slice thickness of 0.8 mm with micro-computed tomography (CT) (RmCT, Rigaku, Tokyo, Japan) (conditions: tube voltage 90.0 kV, tube current 40.0 μA). The DICOM data were reconstructed with software for image analysis (OsiriX version 5.5; Pixmeo, Geneva, Switzerland), and three-dimensional (3D) images of the intercondylar lesion were reconstructed from CT data by a volume-rendering technique. Measurement of the tibial bony prominence was achieved while visualizing the tibial plateau in the axial plane (Figure 2(b)).

Under the reconstructed 3D image, the distances from the AF and PF to the center of each fiber were measured using a marker, and these were defined as AM–AF, ACL–AF, PL–AF, AM–PF, ACL–PF and PL–PF, respectively (Figure 3(a), (b)). To evaluate the positional relationship at the anterior part of intercondylar area, located anterior to the medial and lateral intercondylar tubercles (MIT/LIT), measurements of the location of each point were obtained using a square grid model drawn over the superior view of the intercondylar area by modifying the method described by Kodama et al. [19]. For the square grid setting, the first line was drawn adjacent and parallel to the medial intercondylar ridge (MIR). The second line passed through the intersection between the MIR and anterior ridge [13], the third line connected to the anterior border of the tibial ridge (TR) of the ACL [2], and a perpendicular line from each line was drawn through the first line. The fourth line was drawn perpendicular to the second

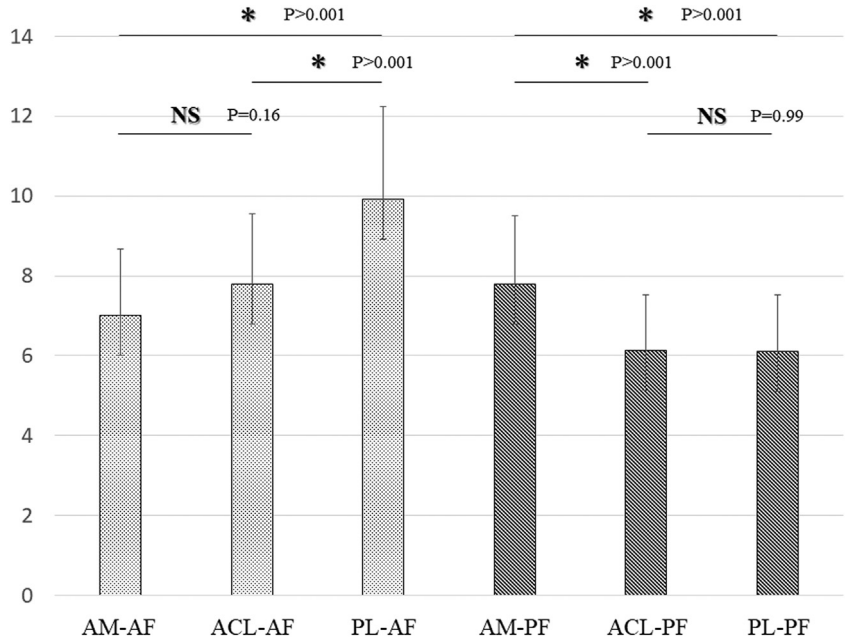

Figure 3. Distance between each anatomical anterior cruciate ligament (ACL) footprint and anterior/posterior fiber insertions. AF, anterior fiber; AM, anteromedial bundle; PF, posterior fiber; PL, posterolateral bundle.

and third lines and connected to the lateral border of the LIT. Utilizing a grid surrounded by these four lines, we verified the relative position of each marked point (Figure 3(c)). Each anatomical insertion and footprint was measured from the anterior and medial border of each reference line and expressed as a percentage of the total depth and width of the grid (Figure 3(d)).

2.3. Statistical analysis

All image measurements were conducted twice by two experienced orthopedic surgeons (SK and KT). Intraclass and interclass correlations were calculated to examine the reproducibility of the measurements. Mean ± standard deviation and 95% confidence interval of each distance and positional parameter were calculated. Each distance was then compared using the Bonferroni test and unpaired *t*-test. The morphological agreement between the observers was quantified using Fleiss' kappa. Referencing power analyses that were reported in similar studies, we performed our own power analysis to indicate a sample size of 35 for addressing our questions in this study (51, 33 and 16% for each shape type, Cohen's kappa statistic = 0.73, significance level = 0.05 and power = 0.80) [7,20].

3. Results

The coefficients of the distance and dimension were 0.90 and 0.84, respectively. The AM–AF, ACL–AF, and PL–AF were 7.4 ± 1.5 mm, 8.2 ± 1.4 mm, and 10.3 ± 1.9 mm, respectively, and the AM–F, ACL–PF, PL–PF were 8.0 ± 1.3 mm, 6.3 ± 1.0 mm, and 6.3 ± 1.2 mm, respectively (Table 1, Figure 4). There was no significant difference between the AM–AF and ACL–AF ($P = 0.16$), but both were significantly shorter than the PL–AF (both $P < 0.001$). There was also no significant difference between ACL–PF and PL–PF ($P = 0.99$), which were significantly shorter than AM–PF (both $P < 0.001$). Of the 33 knees included in this study, 15 knees (45.5%) were classified as triangle type, 18 (54.5%) were classified as oval type, and none were classified as C-shaped type. The reliability of classification was 0.55. There was no significant difference in terms of the PL–AF between morphologies ($P = 0.13$), but compared to the triangular type, both the AM–AF and ACL–AF were significantly shorter in the oval type ($P < 0.001$, $P = 0.004$, respectively) (Table 2). Moreover, the AM–PF, ACL–PF, and PL–PF showed no significant differences between morphologies ($P = 0.39$, 0.09, and 0.4, respectively). Additionally, the center of each footprint and AF/PF insertion in the configured grid are shown in Tables 3, 4, and Figure 5 sections. Compared to the oval type, the AF of the triangle type was positioned significantly anteriorly and laterally ($P = 0.03$, 0.01, respectively), while the PF was located more anteriorly ($P = 0.009$) despite no significant difference in its mediolateral positioning ($P = 0.14$). Aside from two cases, the center of the outer/posterior fiber was located laterally to the ML center of the grid.

4. Discussion

The most important finding of our study was that the AM and ACL center were significantly closer to the AF insertion compared to the PL center, and the ACL and PL center were significantly closer to the PF compared to the AM center. Although the AF was in closer proximity to the AM and ACL center in the oval type compared to the triangular type, there was no difference between morphologies of the footprints in PF. The same tendency was also confirmed in the evaluation of their relative positions. ALMR insertions were for the most part located laterally to the midpoint between the MIT and LIT, indicating that there is a risk of damage if these boundaries are crossed. These results suggest that the injury site of the ALMR insertion can be different according to where the bone tunnel is constructed, and that the proximity of ACL tibial footprint to the ALMR insertion can vary between cases, which would imply that the risk of damaging the ALMR insertion would also differ on a case-by-case basis.

Recently, there has been a growing interest in the proximity of the ACL tibial footprint and the ALMR, and detailed studies from a variety of perspectives have been conducted. Several reports have stated that the boundary between the ACL and the ALMR is macroscopically indistinct, and LaPrade et al. report that 40.7% of the ACL and 63.2% of the anterior horn of the lateral

Table 1
The distance between each attachment of fiber bundles and anterior fiber (AF)/posterior fiber (PF) of anterolateral meniscal root insertions.

	Mean (range)	95% CI
AM–AF (mm)	7.4 ± 1.5 (4.1–10.4)	6.9–8.0
ACL–AF (mm)	8.2 ± 1.4 (5.0–10.9)	7.7–8.7
PL–AF (mm)	10.3 ± 1.9 (5.9–14.1)	9.6–11.0
AM–PF (mm)	8.0 ± 1.3 (5.6–12.1)	7.5–8.5
ACL–PF (mm)	6.3 ± 1.0 (4.0–9.1)	5.9–6.7
PL–PF (mm)	6.3 ± 1.2 (4.0–8.5)	5.8–6.7

ACL, anterior cruciate ligament; AM, anteromedial bundle; CI, confidence interval; PL, posterolateral bundle.

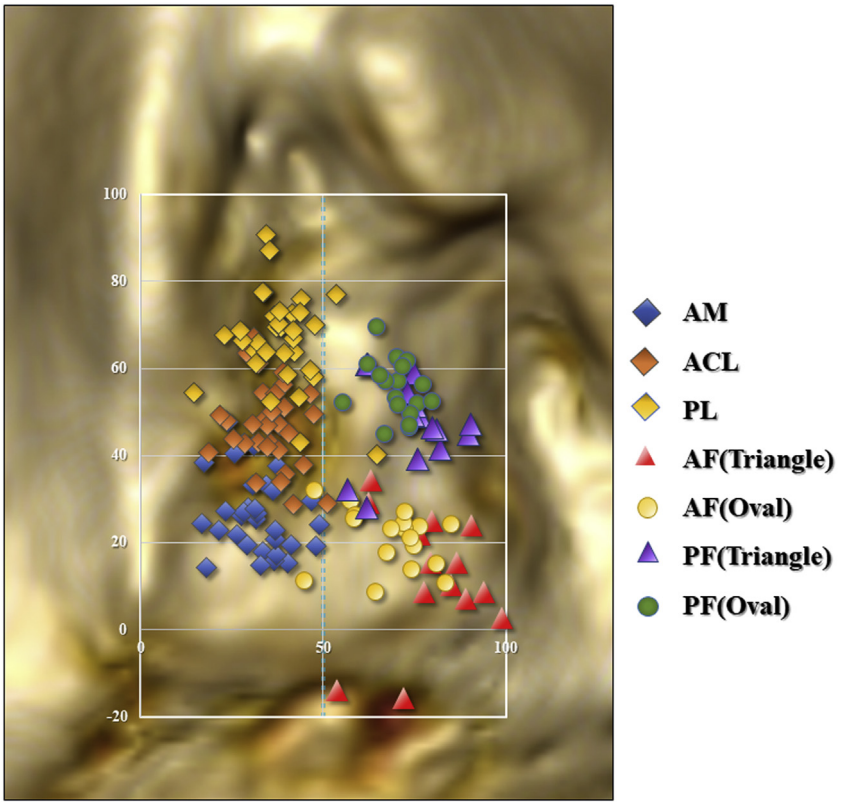

Figure 4. Scaled scatter diagram comparing the centers of each anterior cruciate ligament (ACL) footprint and anterior/posterior fiber insertions. Excluding two cases, the anterior fiber (AF)/posterior fiber (PF) insertion was located laterally to the ML center of the medial and lateral intercondylar tubercles. Blue square, center of anteromedial bundle (AM) footprint; orange square, center of ACL footprint; yellow square, center of posterolateral bundle (PL) footprint; red circle, center of AF insertion; green circle, PF, center of PF insertion, red dotted line, center of the medial and lateral intercondylar tubercles line aligned to the anteroposterior axis of the grid. (For interpretation of the references to color in this figure legend, the reader is referred to the web version of this article.)

meniscus overlap [11]. In addition, Steineman et al. conducted detailed evaluations using a scanning electron microscope, and stated that the ACL tibial footprint and ALMR were overlapped by 41% in the coronal direction and 53.9% in the sagittal direction [12]. Furthermore, Fujishiro et al. found that by dividing the anterior horn of the lateral meniscus into outer/inner fibers and establishing a continuity between the ACL and outer fiber, the inner fiber forms the lateral border of the ACL [8]. Although the boundary between the two was macroscopically indistinct, the authors stated that the two can be easily differentiated histologically [8,10]. In our present study, in order to quantitatively evaluate the proximity of the ALMR, many cadavers were evaluated

Table 2
Comparison of the distance between each attachment of fiber bundles and anterior fiber (AF)/posterior fiber (PF) insertions for the anterior cruciate ligament (ACL) tibial insertion morphology.

	Triangular (n = 15)	Oval (n = 18)	
	Mean (range)	Mean (range)	*P*
AM–AF, mm	8.4 ± 1.1 (6.7–10.4)	6.6 ± 1.1 (4.1–9.8)	<0.0001
ACL–AF, mm	9.0 ± 1.4 (6.5–10.9)	7.6 ± 1.1 (5–10.3)	0.004
PL–AF, mm	10.9 ± 2.3 (5.9–14.1)	9.8 ± 1.5 (6.2–12.9)	0.13
AM–PF, mm	7.8 ± 1.3 (5.6–10.6)	8.2 ± 1.2 (6.9–12.1)	0.39
ACL–PF, mm	6.0 ± 1.0 (4.0–8.1)	6.6 ± 0.9 (4.9–9.1)	0.09
PL–PF, mm	6.1 ± 1.4 (4.6–8.5)	6.4 ± 0.9 (4.0–8.3)	0.40

AM, anteromedial bundle; PL, posterolateral bundle.

Table 3
Anteroposterior and mediolateral positions for center of each anterior cruciate ligament (ACL) fiber bundle and anterior fiber (AF)/posterior fiber (PF) attachment within the grid.

	AP position (%)		ML position (%)	
	Mean ± SD (range)	95% CI	Mean ± SD (range)	95% CI
AM	27.2 ± 9.2 (14.1–47.8)	23.9–30.5	31.7 ± 8.1 (16.6–48.8)	28.8–34.6
ACL	46.7 ± 9.1 (28.6–67.2)	43.5–50.0	35.4 ± 7.1 (18.6–51.7)	32.8–37.9
PL	66.5 ± 10.6 (40.3–90.8)	62.8–70.3	38.3 ± 9.0 (14.5–64.6)	36.1–41.5
AF	17.0 ± 11.3 (−15.5 to 34.2)	13.0–21.1	74.0 ± 13.7 (44.7–101.4)	69.1–78.8
PF	51.6 ± 8.7 (28.1–69.3)	48.4–54.7	72.0 ± 8.0 (55.5–90.3)	69.1–74.9

AM, anteromedial bundle; AP, anteroposterior; CI, confidence interval; ML, mediolateral; PL, posterolateral bundle; SD, standard deviation.

under macroscopic analysis. On the articular side, the boundary between the two constructs was indistinct, but by carefully peeling off the meniscus from the bony side, the positioning of main parts in the ALMR could be sufficiently identified.

In recent years, the risk of the ALMR injury in ACL reconstruction has been more frequently reported in the literature [15–17]. A cadaveric study reported that the bone tunnel construction at the center of the ACL footprint decreases the area of ALMR and also decreased its pull-out strength [16], and another study reported that a single-bundle reconstruction constructing a large bone tunnel at the center caused a higher risk of damage to the ALMR compared to double-bundle reconstruction constructing two tunnels in the anterior–posterior direction [15]. In actual clinical practice, Furumatsu et al. reported a case in which the extrusion of the lateral meniscus was caused by damaging the ALMR during ACL reconstruction [18]. In addition, Kodama et al. created a grid in the intercondylar area, and stated that tunnels less than five millimeters from the lateral reference point had an extrusion of the lateral meniscus under postoperative magnetic resonance imaging for double-bundle reconstruction [19]. In our present study, the AM center was positioned near the AF insertion, the PL center and PF insertion were consistently positioned within approximately six millimeters of each other, and the ACL center was in close proximity to both the AF and PF insertions. Considering that the size of the tibial tunnel created during an actual surgery is nine to 10 mm for single-bundle reconstruction, drilling the centers of the AM and PL may cause partial damage to the ALMR attachment, and drilling the ACL center may cause extensive damage. Even double-bundle reconstruction that creates a six- to seven-millimeter bone tunnel would possibly create partial damage to the ALMR insertion in case the bone tunnel is laterally positioned.

The diverse anatomical variation of the ACL tibial footprint is well known [5], and many reports classify the variations as either triangle or oval type [13,14]. In recent years, C-shaped morphologies have also been reported [21]. Although we were unable to confirm a C-shaped morphology in this report, the compositions of morphological types were almost identical to those of previous reports. The interrelationship between the ACL and ALMR varies depending on the morphology of the footprint, and the proximity between AF and center of AM, ACL can especially vary depending on the morphology of the footprint (Figure 5(a), (b)). As predicted, this implies that the risk of damage can also vary according to footprint morphology; thus, a finer calibration of tunnel positioning may be necessary, especially when the drilling position is either in the anterior or center of the tibial footprint.

Table 4
Comparison of anteroposterior and mediolateral positions between tibial footprint morphologies for the center of anterior fiber (AF)/posterior fiber (PF) attachment within the grid.

AP position	AF			PF		
	Triangle (n = 15)	Oval (n = 18)	*P*	Triangle (n = 15)	Oval (n = 18)	*P*
Mean	12.5 ± 14.1	20.8 ± 6.7	0.03	47.3 ± 9.5	55.1 ± 6.4	0.009
Range (%)	−15.5 to 34.2	10.6–31.8		28.1–60.8	44.9–69.3	
95% CI	4.7–20.3	17.5–24.2		42.0–52.6	51.9–58.3	
ML position	AF			PF		
	Triangle (n = 15)	Oval (n = 18)	*P*	Triangle (n = 15)	Oval (n = 18)	*P*
Mean	80.5 ± 13.7	68.5 ± 11.3	0.01	74.3 ± 10.2	70.1 ± 5.8	0.14
Range (%)	53.5–101.4	44.7–83.5		61.7–90.3	55.5–79.9	
95% CI	72.9–88.1	62.9–74.2		68.7–79.8	67.2–73.0	

AP, anteroposterior; CI, confidence interval; ML, mediolateral.

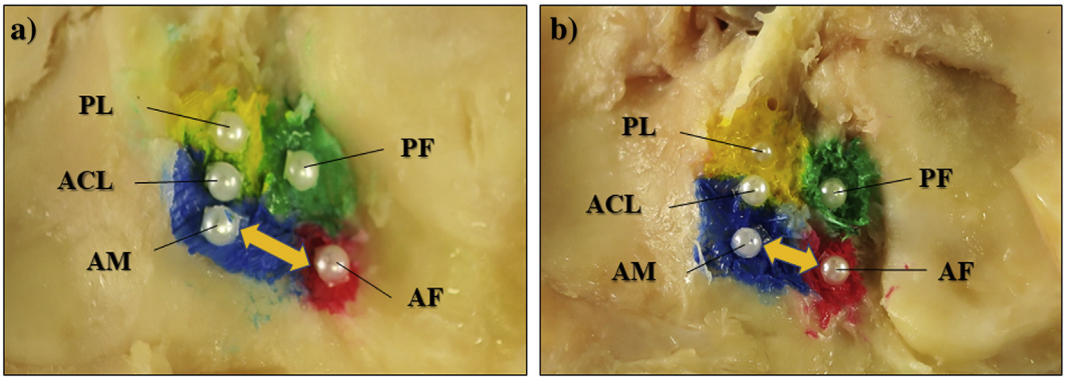

Figure 5. Positional relationship between the center of each fiber bundle and anterior fiber (AF)/posterior fiber (PF) insertions. The positional relationship of the AF differs according to the morphology of the tibial footprint. (a) Triangular type: there is distance between the AF and the center of anteromedial bundle footprint (AM)/center of ACL footprint (ACL). (b) Oval type: there is no distance between the AF and center of the AM/ACL, and the two are in close proximity to each other.

In actual arthroscopic surgery, it is difficult to distinguish the boundary between the ACL and the ALMR. Kusano et al. reported the presence of a small protrusion at the boundary of the ACL–ALMR attachment – the central intercondylar ridge – and stated that the structure is useful in discerning a boundary [10]. However, the bony landmark that they describe is very small, and the protrusion remains very difficult to confirm by arthroscopic observation even if the remnant is extensively resected. In this study, centers of AF/PF insertions were both positioned at 69% for the lower limits of the 95% confidence interval within the square grid. Considering factors such as ease of intraoperative discernibility, individual variation, and safety margins in arthroscopic surgery, we suggested that the midpoint of the MIT and LIT was a good indicator for estimating the boundary and avoiding intraoperative ALMR injury. The MIT/LIT is a bony landmark which can almost certainly be recognized under arthroscopy without remnant removal, and we believe the landmark can be appropriately referenced as an indicator [22].

4.1. Limitations

There are several limitations to our research. The detailed insertion of the ALMR can only be determined histologically. However, it is difficult to histologically evaluate the diverse anatomical variations of the insertion, and what remains important in the clinical practice of arthroscopic surgery is macroscopic quantitative data. In this regard, we believe that our results could provide important information on actual arthroscopic surgery. In this study, we used fixed specimens in place of fresh-frozen cadavers, and the specimens were generally of old age. However, because we carefully selected specimens without osteoarthritis and only evaluated their morphology, we think that the results will not be greatly affected. In addition, all specimens used were of Asian race, and this may have influenced our results. However, since there is little racial variance in the width of the tibial footprint compared to the length, we think that its clinical significance remains unchanged [13,23–26]. In order to conduct a detailed analysis of ALMR, we divided the meniscal root into two parts based on the method of a previous study. However, clinical significance for each part of the ALMR is unclear.

5. Conclusions

In this study, we quantitatively and positionally evaluated the proximity between the ACL footprint and ALMR. The proximity of the ACL tibial footprint and ALMR varies by their detailed parts and footprint morphology, especially for AF insertion. These complex anatomical interrelationships should be considered when determining the position of bone tunnels, and MIT and LIT are useful landmarks in predicting both of their boundaries under arthroscopic surgery.

Declaration of Competing Interest

The authors have no conflicts of interest to disclose.

References

[1] Colombet P, Robinson J, Christel P, Franceschi JP, Djian P, Bellier G, et al. Morphology of anterior cruciate ligament attachments for anatomic reconstruction: a cadaveric dissection and radiographic study. Arthroscopy 2006;22:984–92.
[2] Purnell ML, Larson AI, Clancy W. Anterior cruciate ligament insertions on the tibia and femur and their relationships to critical bony landmarks using high-resolution volume-rendering computed tomography. Am J Sports Med 2008;36:2083–90.
[3] Takahashi M, Doi M, Abe M, Suzuki D, Nagano A. Anatomical study of the femoral and tibial insertions of the anteromedial and posterolateral bundles of human anterior cruciate ligament. Am J Sports Med 2006;34:787–92.
[4] Tsukada H, Ishibashi Y, Tsuda E, Fukuda A, Toh S. Anatomical analysis of the anterior cruciate ligament femoral and tibial footprints. J Orthop Sci 2008;13:122–9.

[5] Edwards A, Bull AM, Amis AA. The attachments of the anteromedial and posterolateral fibre bundles of the anterior cruciate ligament: part 1: tibial attachment. Knee Surg Sports Traumatol Arthros 2007;15:1414–21.
[6] Ferretti M, Doca D, Ingham SM, Cohen M, Fu FH. Bony and soft tissue landmarks of the ACL tibial insertion site: an anatomical study. Knee Surg Sports Traumatol Arthrosc 2012;20:62–8.
[7] Guenther D, Irarrazaval S, Nishizawa Y, Vernacchia C, Thorhauer E, Musahl V, et al. Variation in the shape of the tibial insertion site of the anterior cruciate ligament: classification is required. Knee Surg Sports Traumatol Arthrosc 2017;25:2428–32.
[8] Fujishiro H, Tsukada S, Nakamura T, Nimura A, Mochizuki T, Akita K. Attachment area of fibres from the horns of lateral meniscus: anatomic study with special reference to the positional relationship of anterior cruciate ligament. Knee Surg Sports Traumatol Arthrosc 2017;25:368–73.
[9] Furumatsu T, Kodama Y, Maehara A, Miyazawa S, Fujii M, Tanaka T, et al. The anterior cruciate ligament–lateral meniscus complex: a histological study. Connect Tissue Res 2016;57:91–8.
[10] Kusano M, Yonetani Y, Mae T, Nakata K, Yoshikawa H, Shino K. Tibial insertions of the anterior cruciate ligament and the anterior horn of the lateral meniscus: a histological and computed tomographic study. Knee 2017;24:782–91.
[11] LaPrade CM, Ellman MB, Rasmussen MT, James EW, Wijdicks CA, Engebretsen L, et al. Anatomy of the anterior root attachments of the medial and lateral menisci: a quantitative analysis. Am J Sports Med 2014;42:2386–92.
[12] Steineman BD, Moulton SG, Haut Donahue TL, Fontbote CA, LaPrade CM, Cram TR, et al. Overlap between anterior cruciate ligament and anterolateral meniscal root insertions: a scanning electron microscopy study. Am J Sports Med 2017;45:362–8.
[13] Tensho K, Shimodaira H, Aoki T, Narita N, Kato H, Kakegawa A, et al. Bony landmarks of the anterior cruciate ligament tibial footprint: a detailed analysis comparing 3-dimensional computed tomography images to visual and histological evaluations. Am J Sports Med 2014;42:1433–40.
[14] Ziegler CG, Pietrini SD, Westerhaus BD, Anderson CJ, Wijdicks CA, Johansen S, et al. Arthroscopically pertinent landmarks for tunnel positioning in single-bundle and double-bundle anterior cruciate ligament reconstructions. Am J Sports Med 2011;39:743–52.
[15] Karakasli A, Acar N, Basci O, Karaarslan A, Erduran M, Kaya E. Iatrogenic lateral meniscus anterior horn injury in different tibial tunnel placement techniques in ACL reconstruction surgery — a cadaveric study. Acta Orthop Traumatol Turc 2016;50:514–8.
[16] LaPrade CM, Smith SD, Rasmussen MT, Hamming MG, Wijdicks CA, Engebretsen L, et al. Consequences of tibial tunnel reaming on the meniscal roots during cruciate ligament reconstruction in a cadaveric model, part 1: the anterior cruciate ligament. Am J Sports Med 2015;43:200–6.
[17] Watson JN, Wilson KJ, LaPrade CM, Kennedy NI, Campbell KJ, Hutchinson MR, et al. Iatrogenic injury of the anterior meniscal root attachments following anterior cruciate ligament reconstruction tunnel reaming. Knee Surg Sports Traumatol Arthrosc 2015;23:2360–6.
[18] Furumatsu T, Ozaki T. Iatrogenic injury of the lateral meniscus anterior insertion following anterior cruciate ligament reconstruction: a case report. J Orthop Sci 2018;23:197–201.
[19] Kodama Y, Furumatsu T, Miyazawa S, Fujii M, Tanaka T, Inoue H, et al. Location of the tibial tunnel aperture affects extrusion of the lateral meniscus following reconstruction of the anterior cruciate ligament. J Orthop Res 2017;35:1625–33.
[20] Tashiro Y, Lucidi GA, Gale T, Nagai K, Herbst E, Irrgang JJ, et al. Anterior cruciate ligament tibial insertion site is elliptical or triangular shaped in healthy young adults: high-resolution 3-T MRI analysis. Knee Surg Sports Traumatol Arthrosc 2018;26:485–90.
[21] Siebold R, Schuhmacher P, Fernandez F, Smigielski R, Fink C, Brehmer A, et al. Flat midsubstance of the anterior cruciate ligament with tibial "C"-shaped insertion site. Knee Surg Sports Traumatol Arthrosc 2015;23:3136–42.
[22] Shimodaira H, Tensho K, Akaoka Y, Takanashi S, Kato H, Saito N. Remnant-preserving tibial tunnel positioning using anatomic landmarks in double-bundle anterior cruciate ligament reconstruction. Arthroscopy 2016;32:1822–30.
[23] Kopf S, Pombo MW, Szczodry M, Irrgang JJ, Fu FH. Size variability of the human anterior cruciate ligament insertion sites. Am J Sports Med 2011;39:108–13.
[24] Morgan CD, Kalman VR, Grawl DM. Definitive landmarks for reproducible tibial tunnel placement in anterior cruciate ligament reconstruction. Arthroscopy 1995;11:275–88.
[25] Siebold R, Ellert T, Metz S, Metz J. Tibial insertions of the anteromedial and posterolateral bundles of the anterior cruciate ligament: morphometry, arthroscopic landmarks, and orientation model for bone tunnel placement. Arthroscopy 2008;24:154–61.
[26] Tallay A, Lim MH, Bartlett J. Anatomical study of the human anterior cruciate ligament stump's tibial insertion footprint. Knee Surg Sports Traumatol Arthrosc 2008;16:741–6.